

# Vacuum Localized Structures: Revisiting the Dark Matter Paradigm

**R. Van Nieuwenhove**

Independent researcher (previously at Belgian Nuclear Research Centre SCK-CEN)

E-mail: [rvnieuwe@gmail.com](mailto:rvnieuwe@gmail.com)  
Skipper 27, 2480 Dessel, Belgium

## Abstract

This study presents the mathematical derivation of Vacuum Localized Structures (VLS), gravitationally stable spacetime structures, as an alternative to dark matter. Assuming galaxies are embedded in galactic-sized VLS, the observed flat galaxy rotation curves can be explained without requiring the standard dark matter halo. This concept has been applied to the case of the Milky Way and profiles of density, pressure and rotation velocity have been derived, demonstrating a close correspondence with the observations. The VLS Gaussian density profile naturally explains the flat central density cores observed in dwarf galaxies, providing a compelling solution to the core-cusp problem. Furthermore, the early formation of VLS shortly after the Big Bang offers a framework for understanding the rapid emergence of massive galaxies, addressing the challenges posed by recent James Webb Space Telescope observations. These findings suggest that VLS could serve as both the gravitational scaffolding for galaxy formation and a replacement for cold dark matter, unifying multiple cosmological phenomena under a single theoretical framework.

Keywords: galaxy, vacuum localized structure, rotation curve, dark matter

---

## 1. Introduction

The enigmatic nature of galaxy rotation curves, first observed in the 1970s, remains one of the most compelling puzzles in astrophysics. Measurements of rotational velocities in galaxies exhibit a surprising flatness at large radii, deviating from the expected Keplerian decline. This phenomenon has traditionally been attributed to the presence of unseen mass, commonly referred to as dark matter. However, despite decades of dedicated research, direct detection of dark matter particles has proven elusive [1], motivating alternative explanations rooted in the fundamental physics of gravitation.

In this context, we revisit the concept of gravitational VLS, self-sustaining field configurations governed purely by Einstein's Field Equations (EFE) [2]. Originally introduced by John Archibald Wheeler in 1955, geons ("gravitational electromagnetic entity") were envisioned as stable, localized energy constructs formed from gravitational and electromagnetic fields [3]. However, these geons were primarily considered in small-scale scenarios, often limited by their susceptibility to radiation leakage and other instabilities. Wheeler did not present explicit geon solutions to the vacuum Einstein field equation, a gap which was partially filled by Brill and Hartle in 1964 [4]. In their paper they applied their method to the case of a static spherically symmetric background geometry and found that gravitational waves can remain confined in a region for a time much longer than the region's light-crossing time. This so-called gravitational geon

is generated by a large number of high frequency, small amplitude gravitational waves. The time average of the curvature due to these waves creates the background geometry of the geon, and this background geometry traps the waves for a long time in a region of space called the “active” region.

In this paper, we will investigate another type of solution which is very different in nature from previously investigated types of geons. Here we will focus on a spherically symmetric, stationary VLS with a spatial extension similar to that of galaxies, or even larger. The existence of such VLS was already conjectured in 1998 [5], although a mathematical proof was not provided. Strictly speaking, the only non-trivial, matter-free solutions to the Einstein Field Equations are the Schwarzschild and Kerr spacetimes. Nevertheless, we will here introduce a special (non-zero) stress-energy tensor with an equation of state reminiscent of the vacuum. We find then exact, non-trivial, analytical solutions to the EFE. Imagining that galaxies are embedded within such VLS, we will demonstrate that it is possible to explain the observed, relatively flat, galaxy rotation curves. Further, it will be argued that such galactic sized VLS can play a role in galaxy formation, providing an explanation for the observation of galaxies in the early universe (300 million years after the Big Bang), which are difficult to explain within the standard  $\Lambda$ CDM model [6-8].

## 2. Mathematical VLS description

### 2.1. Einstein Field Equations

We consider a static, spherically symmetric spacetime

$$ds^2 = -e^{2\Phi(r)}c^2dt^2 + e^{2\Lambda(r)}dr^2 + r^2(d\theta^2 + \sin^2\theta d\phi^2). \quad (1)$$

The anisotropic stress–energy tensor is

$$T^\mu{}_\nu = \text{diag}(-\rho c^2, p_r, p_t, p_t). \quad (2)$$

Einstein’s equations

$$G^\mu{}_\nu = \frac{8\pi G}{c^4} T^\mu{}_\nu \quad (3)$$

yield the independent components:

(tt component)

$$\frac{1}{r^2} - e^{-2\Lambda} \left( \frac{1}{r^2} - \frac{2\Lambda'}{r} \right) = \frac{8\pi G}{c^2} \rho. \quad (4)$$

(rr component)

$$-\frac{1}{r^2} + e^{-2\Lambda} \left( \frac{1}{r^2} + \frac{2\Phi'}{r} \right) = \frac{8\pi G}{c^4} p_r. \quad (5)$$

( $\theta\theta$  component)

$$e^{-2\Lambda} \left( \Phi'' + \Phi'^2 - \Phi'\Lambda' + \frac{\Phi' - \Lambda'}{r} \right) = \frac{8\pi G}{c^4} p_t. \quad (6)$$

From the conservation equation

$$\nabla_\mu T^{\mu r} = 0 \quad (7)$$

$$p_r' = -(\rho c^2 + p_r)\Phi' + \frac{2}{r}(p_t - p_r). \quad (8)$$

Solving for  $p_t$ :

$$p_t = p_r + \frac{r}{2}p_r' + \frac{r}{2}(\rho c^2 + p_r)\Phi' \quad (9)$$

We now assume a weak and slowly varying gravitational field, so that

$$|\Phi| \ll 1, \quad |\Lambda| \ll 1, \quad r|\Phi'| \ll 1, \quad r|\Lambda'| \ll 1, \quad (10)$$

and all products of small quantities are neglected. The metric functions are expanded as

$$\begin{aligned} e^{2\Phi} &\simeq 1 + 2\Phi, & e^{2\Lambda} &\simeq 1 + 2\Lambda, \\ e^{-2\Lambda} &\simeq 1 - 2\Lambda. \end{aligned} \quad (11)$$

Keeping only terms linear in  $\Phi$  and  $\Lambda$ , the Einstein equations reduce to

(tt) component

$$\frac{2\Lambda'}{r} + \frac{2\Lambda}{r^2} = \frac{8\pi G}{c^2} \rho. \quad (12)$$

(rr) component

$$\frac{2\Phi'}{r} - \frac{2\Lambda}{r^2} = \frac{8\pi G}{c^4} p_r. \quad (13)$$

( $\theta\theta$ ) component

$$\Phi'' + \frac{2\Phi'}{r} - \frac{\Lambda'}{r} = \frac{8\pi G}{c^4} p_t. \quad (14)$$

Multiply Equation (12) by  $r^2$ :

$$2r\Lambda' + 2\Lambda = \frac{8\pi G}{c^2} \rho r^2. \quad (15)$$

Recognising

$$\frac{d}{dr}(r\Lambda) = r\Lambda' + \Lambda, \quad (16)$$

we obtain

$$\frac{d}{dr}(r\Lambda) = \frac{4\pi G}{c^2} \rho r^2. \quad (17)$$

we obtain

$$\frac{d}{dr}(r\Lambda) = \frac{4\pi G}{c^2} \rho r^2. \quad (18)$$

From Equation (13)

$$r\Phi' - \Lambda = \frac{4\pi G}{c^4} p_r r^2, \quad (19)$$

hence

$$\Lambda = r\Phi' - \frac{4\pi G}{c^4} p_r r^2. \quad (20)$$

Insert this into Equation (16)

$$\frac{d}{dr} \left( r^2 \Phi' - \frac{4\pi G}{c^4} p_r r^3 \right) = \frac{4\pi G}{c^2} \rho r^2. \quad (21)$$

Expanding:

$$\frac{d}{dr} (r^2 \Phi') - \frac{4\pi G}{c^4} \frac{d}{dr} (p_r r^3) = \frac{4\pi G}{c^2} \rho r^2. \quad (22)$$

Divide by  $r^2$ :

$$\frac{1}{r^2} \frac{d}{dr} (r^2 \Phi') = \frac{4\pi G}{c^2} \rho + \frac{4\pi G}{c^4} \frac{1}{r^2} \frac{d}{dr} (p_r r^3). \quad (23)$$

The left-hand side is the spherical Laplacian:

$$\nabla^2 \Phi = \frac{1}{r^2} \frac{d}{dr} (r^2 \Phi'). \quad (24)$$

*Consistency from the  $\theta\theta$  Equation*

Multiply Equation (14) by  $r$ :

$$r\Phi'' + \Phi' - \Lambda' = \frac{8\pi G}{c^4} p_t r. \quad (25)$$

Since

$$\frac{d}{dr} (r\Phi') = r\Phi'' + \Phi', \quad (26)$$

this gives

$$\Lambda' = \frac{d}{dr} (r\Phi') - \frac{8\pi G}{c^4} p_t r. \quad (27)$$

Differentiate Equation (20)

$$\Lambda' = \frac{d}{dr} (r\Phi') - \frac{4\pi G}{c^4} \frac{d}{dr} (p_r r^2). \quad (28)$$

Equating Equations (27) and (28)

$$\frac{d}{dr} (p_r r^2) = 2p_t r, \quad (29)$$

or

$$\frac{dp_r}{dr} + \frac{2}{r}(p_r - p_t) = 0. \quad (30)$$

This is the weak-field anisotropic equilibrium relation.

Using Equation (30),

$$\frac{d}{dr}(p_r r^3) = r^3 \frac{dp_r}{dr} + 3r^2 p_r = r^2(p_r + 2p_t). \quad (31)$$

Insert into Equation (23),

$$\nabla^2 \Phi = \frac{4\pi G}{c^2} \rho + \frac{4\pi G}{c^4} (p_r + 2p_t). \quad (32)$$

Restoring the Newtonian potential  $\Phi_N = c^2 \Phi$ :

$$\nabla^2 \Phi_N = 4\pi G \left( \rho + \frac{p_r + 2p_t}{c^2} \right). \quad (33)$$

This is the Poisson equation with the Tolman active gravitational mass density for anisotropic stresses.

With spherical symmetry,

$$\nabla^2 \Phi = \frac{1}{r^2} \frac{d}{dr} (r^2 \Phi'(r)). \quad (34)$$

We define

$$\rho(r) = \rho_0 e^{-r^2/R^2}, \quad (35)$$

$$p_r = -\alpha \rho c^2, p_t = -\alpha \rho c^2 + \alpha c^2 \frac{r^2}{R^2} \rho. \quad (36)$$

Hence

$$p_r + 2p_t = -3\alpha \rho c^2 + 2\alpha c^2 \frac{r^2}{R^2} \rho. \quad (37)$$

So the active source becomes

$$\rho_{\text{eff}}(r) = \rho + \frac{p_r + 2p_t}{c^2} = \rho_0 \left( 1 - 3\alpha + 2\alpha \frac{r^2}{R^2} \right) e^{-r^2/R^2}. \quad (38)$$

Equation (34) becomes

$$\frac{1}{r^2} \frac{d}{dr} (r^2 \Phi') = \frac{4\pi G}{c^2} \rho_0 \left( 1 - 3\alpha + 2\alpha \frac{r^2}{R^2} \right) e^{-r^2/R^2}. \quad (39)$$

Multiply Equation (39) by  $r^2$  and integrate from 0 to  $r$ :

$$r^2 \Phi'(r) = \frac{4\pi G \rho_0}{c^2} \int_0^r (1 - 3\alpha + 2\alpha \frac{s^2}{R^2}) s^2 e^{-s^2/R^2} ds. \quad (40)$$

Define  $x = r/R$ ,  $u = s/R$ . Then

$$r^2 \Phi'(r) = \frac{4\pi G \rho_0 R^3}{c^2} \int_0^x (1 - 3\alpha + 2\alpha u^2) u^2 e^{-u^2} du. \quad (41)$$

Working out the integral,

$$r^2 \Phi'(r) = \frac{4\pi G \rho_0 R^3}{c^2} \frac{1}{4} \left\{ \sqrt{\pi} R^3 \operatorname{erf}\left(\frac{r}{R}\right) - 2r(2\alpha r^2 + R^2) e^{-\frac{r^2}{R^2}} \right\} \quad (42)$$

Thus

$$\Phi'(r) = \frac{\pi G \rho_0 R^3}{c^2 r^2} \left\{ \sqrt{\pi} \operatorname{erf}\left(\frac{r}{R}\right) - 2r \left( \frac{2\alpha r^2 + R^2}{R^3} \right) e^{-\frac{r^2}{R^2}} \right\} \quad (43)$$

Introducing  $x = r/R$ , one has

$$\frac{d\Phi}{dr} = \frac{1}{R} \frac{d\Phi}{dx}. \quad (44)$$

The acceleration (or force on a unit test mass) is then given by

$$\frac{d\Phi}{dx} c^2 = 4\pi G \rho_0 R^2 \left[ \frac{\sqrt{\pi}}{4x^2} \operatorname{erf}(x) - \left( \frac{1}{2x} + \alpha x^3 \right) e^{-x^2} \right]. \quad (45)$$

The potential is then given by

$$\Phi(x) = \frac{\pi G \rho_0 R^2}{c^2} \left( 2 \alpha e^{-x^2} (x^2 + 1) - \frac{\sqrt{\pi} \operatorname{erf}(x)}{x} \right) + \text{constant} \quad (46)$$

### ***Circular velocity profile***

In the weak-field and non-relativistic limit, the radial acceleration of a test particle is

$$a_r(r) = -\frac{GM(r)}{r^2} - c^2 \frac{d\Phi}{dr}, \quad (47)$$

where  $M(r)$  is the enclosed ordinary (baryonic) mass and  $\Phi(r)$  is the gravitational potential generated by the vacuum localised structure.

The circular velocity profile can be written as

$$V(x) = \sqrt{\frac{GM(r)}{Rx} + x c^2 \frac{d\Phi}{dx}}. \quad (48)$$

## **2.2. Total mass of the VLS**

The mass that controls the external field is

$$M_{\text{eff}} = 4\pi \int_0^\infty \rho_{\text{eff}}(r) r^2 dr. \quad (49)$$

For our Gaussian model with  $p_r = -\alpha\rho c^2$ , one finds

$$\rho_{\text{eff}}(r) = \rho_0 \left(1 - 3\alpha + 2\alpha \frac{r^2}{R^2}\right) e^{-r^2/R^2}. \quad (50)$$

Carrying out the integral explicitly, one finds that all  $\alpha$ -dependence cancels, and

$$M_{\text{eff}} = \pi^{3/2} \rho_0 R^3. \quad (51)$$

### 2.3. Choice of the equation of state

The parameter  $\alpha$  controls the relation between the radial pressure and the energy density,  $p_r = -\alpha\rho c^2$ , and therefore determines the relative importance of vacuum-like stresses in the interior of the structure. In the present model, the effective gravitational source entering the weak-field equation is the Tolman combination  $\rho_{\text{eff}} = \rho + p_r/c^2 + 2p_t/c^2$ . For a Gaussian density profile one finds  $\rho_{\text{eff}}(r) = \rho_0(1 - 3\alpha + 2\alpha r^2/R^2) e^{-r^2/R^2}$ . This shows that the central active density is  $\rho_{\text{eff}}(0) = \rho_0(1 - 3\alpha)$ . For  $\alpha > 1/3$  the core becomes gravitationally repulsive, whereas for  $\alpha < 1/3$  the structure behaves as an ordinary attractive mass distribution. The value  $\alpha = 1/3$  is therefore critical: the central active density vanishes, the force is neither attractive nor repulsive at the origin, and the gravitational field is generated entirely by a surrounding shell. This choice excludes an unphysical repulsive core while still allowing nontrivial vacuum stresses to shape the interior field. Interestingly,  $\alpha = 1/3$  also corresponds to the equation of state of an isotropic radiation fluid,  $p = \rho c^2/3$ , although the present configuration remains intrinsically anisotropic. In this sense,  $\alpha = 1/3$  represents a natural boundary between matter-like and vacuum-dominated regimes and provides a minimal vacuum-localised structure with purely attractive gravity.

A common misconception in gravitational physics is that a negative radial pressure, such as the equation of state (equation (19)), necessarily leads to instability. While negative pressure is often associated with repulsive effects in cosmology, in localized gravitational systems, it can contribute to a stable equilibrium when properly balanced. For instance, the Tolman-Oppenheimer-Volkoff (TOV) equation describes equilibrium in relativistic stars, allowing stable configurations with anisotropic pressures, including negative radial pressure in certain regimes [9][10]. Additionally, various stable gravitational structures exhibit regions of negative pressure. A key example is the gravastar model [10], in which an interior de Sitter-like vacuum state ( $p = -\rho c^2$ ) is enclosed by a thin shell, maintaining a stable structure without collapse. Similarly, traversable wormhole solutions require exotic matter with negative pressure to support their throats [11][12], yet under appropriate conditions, such configurations can be dynamically stable. Furthermore, cosmological de Sitter space, which dominates the large-scale universe today due to dark energy ( $p = -\rho c^2$ ), is itself a maximally symmetric and stable solution of Einstein's equations [13]. These examples demonstrate that negative pressure does not inherently lead to instability and can instead be a key ingredient in constructing equilibrium configurations in General Relativity.

It is interesting to note that we are still free in the choice of the energy density at the origin, as well as in the value of the scale length  $R$  in the Gaussian energy density profile. So, these solutions can describe very small entities (scale of atoms) to very large entities (scale of galaxies or larger). Also, it is very likely that solutions, similar to this one, can be found in which the VLS rotates.

### 3. Application to the Milky Way

In the following we will imagine that our galaxy is embedded in a VLS, extending beyond the galaxy. As an example, we will take the case of the Milky Way (MW).

There is still a significant uncertainty in the total mass of the MW, and here we will consider some reasonable values for total, baryonic and bulge mass only for the sake of providing an idea of the effect of the geon on the galaxy rotation curve. Our aim is thus not to provide a detailed modelling of the MW. On the other hand, there are recent rotation curve results by the Gaia DR3 measurements [17] which we will use as a guidance. These results show rotation velocities of the order of 230 km/s, some decline beyond 15 kpc and a pronounced decline beyond 19 kpc. In our very simplistic model, we will use here a uniform (baryonic mass) of  $4.6 \cdot 10^{10} M_{\odot}$  up to a radius of 4 kpc. If we assume for instance a total mass of the MW of  $2.26 \cdot 10^{11} M_{\odot}$  and a baryonic mass  $4.6 \cdot 10^{10} M_{\odot}$  we will choose the mass of the VLS to be the difference between the two, namely  $1.8 \cdot 10^{11} M_{\odot}$ . Using the equation for the total mass of the VLS (Equation 36), we obtain a central density of  $3 \cdot 10^{-21} \text{ kg/m}^3$ . Thus, the VLS mass takes the roll of “dark matter”. Then we chose a suitable scale length (R) of the Gaussian energy density profile, and we adjusted the central density such as to obtain the required total mass of the VLS. The scale length in this case should be somewhere between 8 and 12 kpc and in what follows, we choose the value  $R = 9 \text{ kpc}$ . In fact, at this point, we use it as a fitting parameter to the MW rotation curve. However, this might also hint to a connection between the mass accumulated in the VLS (see next chapter) and the properties of the VLS.

The calculated pressure profiles are shown in Figure 1. Note the region in which the tangential pressure changes sign.

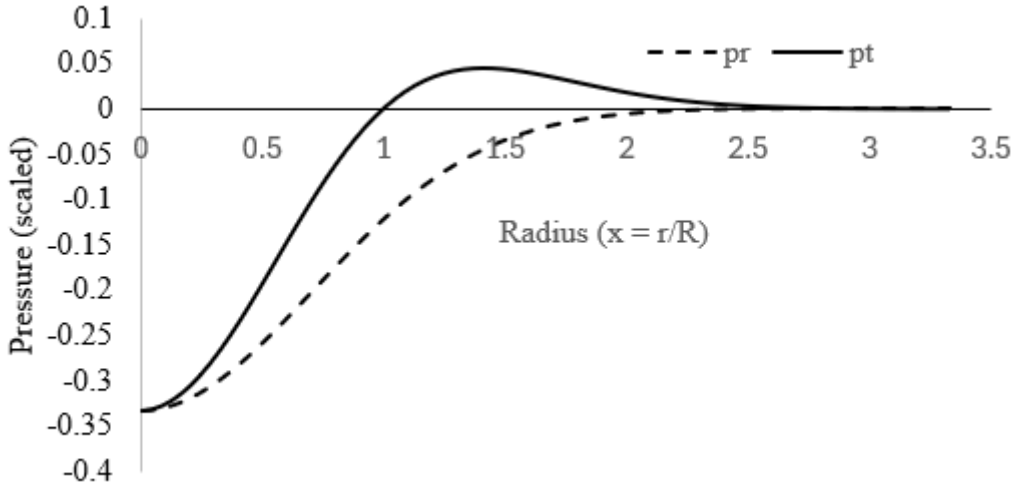


**Figure 1.** Radial ( $p_r$ ) and tangential ( $p_t$ ) pressure profiles of the VLS. The pressure, in units of Pa, is obtained by multiplying the vertical scale by  $\alpha \rho_0$ .

The force profile (based on Equation (45)) induced by the VLS is shown in Figure 2.



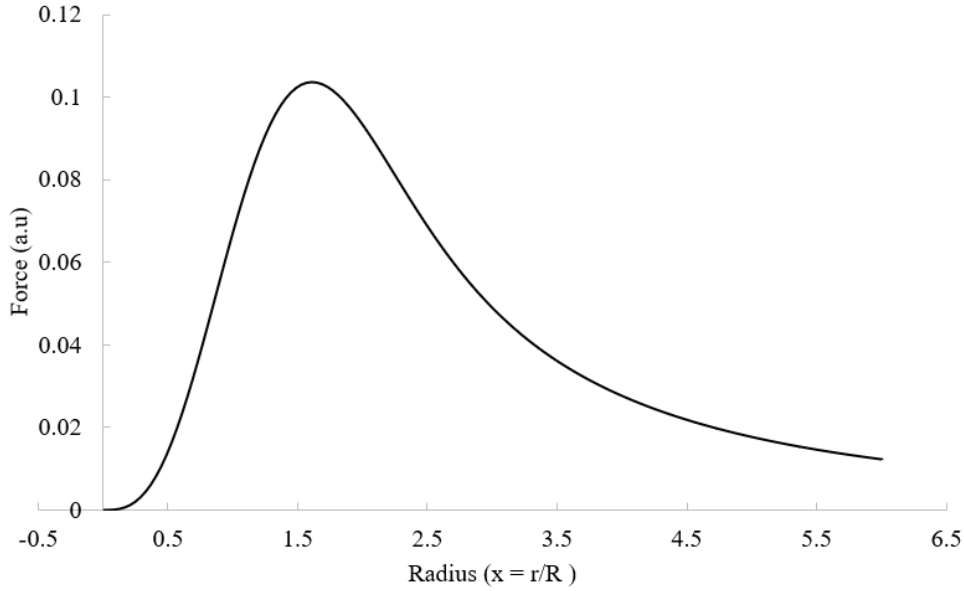


**Figure 2.** Force profile as induced by the VLS. A positive force corresponds to a force towards the center.

Finally, the impact of the VLS on the Milky Way rotation curve (simplistic model) is shown in Figure 3. The additional mass of the VLS results in a relatively flat rotation curve and a decline in the region 15-20 kpc (in agreement with recent observations [17]).

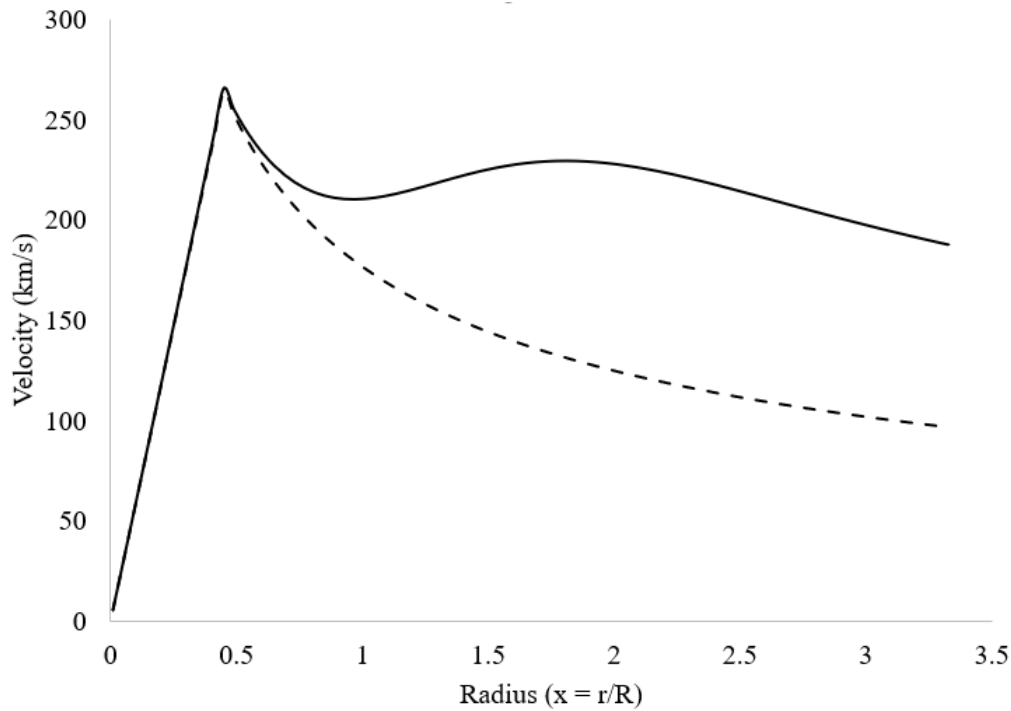


**Figure 3.** Calculated velocity profiles for the Milky Way (simplistic model), showing the Newtonian decay and the relatively flat profiles obtained by the additional force of the VLS.

#### 4. Early galaxy formation and the role of VLSs

The  $\Lambda$ CDM model predicts a hierarchical structure formation process. Dark matter halos form first, through gravitational collapse, providing the scaffolding for baryonic matter to cool and condense into stars and galaxies. However, recent observations from the James Webb Space Telescope (JWST) of massive, mature galaxies at only 250–300 million years after the Big Bang seem to challenge this scenario [18].

The rate of star formation in these galaxies appears inconsistent with the cooling timescales of baryonic gas expected under the  $\Lambda$ CDM model. These galaxies show signs of well-developed morphologies, such as disk-like or compact structures, which are surprising given the chaotic environments expected during early galaxy formation.

VLSs, hypothesized as localized configurations of spacetime, offer an alternative mechanism for structure formation. Unlike dark matter, VLS are fundamentally gravitational phenomena and may have unique properties that make them ideal candidates for explaining early galaxy formation.

In this hypothesis, VLS could form very early in the universe's history, shortly after the inflationary phase ended ( $\approx 10^{-32}$  seconds). During this period, quantum fluctuations in the spacetime fabric—amplified by inflation—could generate regions of intense curvature. These regions might stabilize into VLS through quantum gravitational effects. Importantly, VLS could form seconds to minutes after the Big Bang, far earlier than the formation of large dark matter halos (between 100000 yr to 300 Myr years after the Big Bang). VLS forming almost immediately after inflation, could begin clustering well before recombination. Once baryonic matter decoupled from radiation, VLS would already have deep potential wells in place, potentially allowing them to attract baryonic matter more efficiently than dark matter halos. This earlier gravitational influence might explain how galaxies could form more rapidly and maturely than expected under the standard dark matter model.

The size and "depth" of a VLS (related to its curvature profile and energy density) could determine the amount of baryonic matter it captures. This provides a physical basis for the observed relation between galaxy size and mass.

#### 5. VLS as a solution to the cusp-core problem

The Navarro-Frenk-White (NFW) profile [19], which describes the density of dark matter halos based on simulations, predicts a cuspy central density scaling as  $1/r$ . At small radii, this results in a steep rise in the density near the halo center. In contrast, observations of dwarf galaxies and low-surface-brightness galaxies often show a core, where the density flattens to a roughly constant value near the center [20]. This discrepancy challenges the validity of the standard cold dark matter model or suggests that additional physical processes (e.g., baryonic feedback, alternative dark matter models, or VLS) are needed to explain the observations [21]. One of the most promising solutions to this cold dark matter issue is the stellar feedback mechanism but it seems to be only designed for gas-rich dwarfs, while the problem still remains for gas-poor dwarf spheroidal galaxies. Here, VLS with a Gaussian density profile could provide a natural solution since the gradient of the density becomes zero at the centre.

## 6. Discussion

The VLS solutions rely implicitly on assumptions about the quantum vacuum's properties. While the vacuum is often treated as homogeneous and isotropic, its complexity at microscopic scales suggests the potential for anisotropic effects, such as direction-dependent pressures. These effects could play a significant role in the stability and structure of VLS and might have observable consequences in galaxy dynamics. Understanding the interplay between these effects and the broader cosmic environment remains an intriguing direction for future research.

VLS also offer testable predictions that could distinguish them from standard dark matter models. Their smooth density profiles may produce gravitational lensing patterns and rotation curves subtly different from those predicted by dark matter halos with Navarro-Frenk-White profiles. Additionally, their role in early galaxy formation could leave imprints on the large-scale structure of the universe or in the properties of high-redshift galaxies observed by telescopes like the James Webb Space Telescope.

Their behavior across different scales, ranging from dwarf galaxies to galaxy clusters, requires deeper analysis. Integrating VLS into the broader cosmological framework, particularly in relation to dark energy and cosmic expansion, is also an open question.

The concept of vacuum localised structures is not limited to spherical symmetry. The same theoretical framework naturally allows for cylindrically symmetric configurations, corresponding to extended, filament-like vacuum structures. This is particularly intriguing in light of the observed cosmic web, where matter is distributed along vast filaments connecting clusters and superclusters of galaxies. In such a picture, cosmic filaments would not merely be passive concentrations of dark matter, but could represent gravitationally active vacuum structures that shape the large-scale geometry of matter and influence the formation, motion, and alignment of galaxies along preferred directions. Cylindrical VLS would provide a natural mechanism for long-range gravitational organisation without requiring particulate dark matter to be locally concentrated within the filaments themselves. A systematic analysis of cylindrically symmetric VLS solutions and their gravitational properties will be developed in a forthcoming work.

## 7. Conclusions

It has been shown that a VLS type solution exists to the Einstein Field Equations with a Gaussian density profile and for which the radial pressure is minus one third of the energy density, being reminiscent of a vacuum equation of state. Real VLS solutions could exist within the framework of modified or extended gravity theories. Such galactic sized VLS can take over the role of dark matter, being distributed gravitational structures with a significant mass content. It has been shown that the observed relatively flat galaxy rotation curves can be explained when considering the galaxies to be embedded in large VLS. In particular, the rotation curve for the Milky Way has been modelled using a simple baryonic mass profile embedded in a VLS. Besides explaining the flat rotation curves, the VLS concept can also offer an explanation to the observation of mature galaxies in the early universe, and it offers also a solution to the core-cusp problem in gas-poor dwarf spheroidal galaxies. Finally, cylindrical VLS could represent filaments of the large-scale cosmic web.

**ORCID ID** Rudi Van Nieuwenhove : <http://orcid.org/0000-0003-1265-8718>

## References

- [1] Aalbers J et al 2023 LUX-ZEPLIN Collaboration, First Dark Matter Search Results from the LUX-ZEPLIN (LZ) Experiment, *Phys. Rev. Lett.* **131** 041001
- [2] Misner C W Thorne K S and Wheeler J A *Gravitation*. W. H. Freeman and Company, 1973
- [3] Wheeler J A 1955 Geons *Phys. Rev.* **97.2** 511-36
- [4] Brill D R and Hartle J B 1964 Method of the Self-Consistent Field in General Relativity and its Application to the Gravitational Geon *Phys. Rev.* **135** B271
- [5] Van Nieuwenhove R 1998 Is the missing mass really missing? *Astron. Astrophys. Trans.* **16** (1) 37-40
- [6] Sabti N Muñoz J B Kamionkowski M 2024 Insights from HST into Ultramassive Galaxies and Early-Universe Cosmology *Phys. Rev. Lett.* **132** 061002
- [7] Vagnozzi S, Smoot G F and Visinelli L 2023 Early Galaxies and Early Dark Energy: A Unified Solution to the Hubble Tension, *Mon. Not. R. Astron. Soc.* **533** 3923–3933
- [8] Gupta R (2023) JWST Early Universe Observations and  $\Lambda$ CDM Cosmology, *Mon. Not. R. Astron. Soc.*, **524** 3385–91
- [9] Tolman R. C. *Relativity, Thermodynamics, and Cosmology*, Dover (1987)
- [10] Mazur P. & Mottola E. *Gravitational Condensate Stars: An Alternative to Black Holes*, arXiv:gr-qc/0109035
- [11] Morris M. S. & Thorne K. S., *Wormholes in Spacetime and Their Use for Interstellar Travel: A Tool for Teaching General Relativity*, *Am. J. Phys.* **56**, 395 (1988)
- [12] Lobo F. S. N. *Stable Phantom Energy Traversable Wormholes*, *Phys. Rev. D* **71**, 084011 (2005)
- [13] Carroll S. M. *Spacetime and Geometry: An Introduction to General Relativity*, Addison-Wesley (2004), Section 8.4.
- [14] Riazi N *et al* 2016 Exact anisotropic solutions of the generalized TOV equation *Can. J. Phys.* **94**(10), 996–1005
- [15] Babaei A. and Vakili B 2024 Scalar field cosmology: Classical and quantum viewpoints *Int. J. Theor. Phys.* **63**, 2751–2774
- [16] De Felice A and Tsujikawa S 2010  $f(R)$  theories *Living Rev. in Relativ.* **13**, 3
- [17] Beordo W, Crosta M and Lattanzi M G 2024 Exploring Milky Way rotation curves with Gaia DR3: a comparison between  $\Lambda$ CDM, MOND, and General Relativistic approaches. *JCAP* 2024(12), 024
- [18] Laursen P 2023 Galaxy Formation from a Timescale Perspective *Astron. Astrophys.*, in press, (arXiv:2309.02486)
- [19] Navarro, J F, Frenk C S, White S D M 1996 The Structure of Cold Dark Matter Halos *Astrophys. J.*, **462** 563-75 (arXiv:astro-ph/9508025)
- [20] Oman K 2015 The unexpected diversity of dwarf galaxy rotation curves, *Monthly Notices of the Royal Astronomical Society*, **452** (4) 3650-3665
- [21] Boldrini P 2022 The Cusp-Core Problem in Gas-Poor Dwarf Spheroidal Galaxies, *Galaxies*, **10** (1)